Letter

Synthesis and SAR studies of 1H-pyrrolo[2,3-b]pyridine-2-carboxamides as phosphodiesterase 4B (PDE4B) inhibitors

Anish K Vadukoot, Swagat Sharma, Christopher D Aretz, Sushil Kumar, Nagsen Gautam, Yazen Alnouti, Amy L Aldrich, Cortney E. Heim, Tammy Kielian, and Corey R. Hopkins

ACS Med. Chem. Lett., **Just Accepted Manuscript** • DOI: 10.1021/acsmedchemlett.9b00369 • Publication Date (Web): 24 Jan 2020

Synthesis and SAR studies of 1*H*-pyrrolo[2,3-*b*]pyridine-2-carboxamides as phosphodiesterase 4B (PDE4B) inhibitors

Anish K. Vadukoot[1], Swagat Sharma[1], Christopher D. Aretz[1], Sushil Kumar[1], Nagsen Gautam[1], Yazen Alnouti[1], Amy L. Aldrich[2], Cortney E. Heim[2], Tammy Kielian[2], and Corey R. Hopkins[1,*]

[1]Department of Pharmaceutical Sciences, College of Pharmacy, University of Nebraska Medical Center, Omaha, NE 68198

[2]Department of Pathology and Microbiology, College of Medicine, University of Nebraska Medical Center, Omaha, NE 68198.

KEYWORDS: 1H-pyrrolo[2,3-b]pyridine-2-carboxamide, PDE4B, phosphodiesterase 4, scaffold hopping.

ABSTRACT: Herein we report the synthesis, SAR, and biological evaluation of a series of 1*H*-pyrrolo[2,3-*b*]pyridine-2-carboxamide derivatives as selective and potent PDE4B inhibitors. Compound **11h** is a PDE4B preferring inhibitor and exhibited acceptable *in vitro* ADME and significantly inhibited TNF-α release from macrophages exposed to pro-inflammatory stimuli (*i.e.*, lipopolysaccharide and the synthetic bacterial lipopeptide Pam3Cys). In addition, **11h**, was selective against a panel of CNS receptors and represents an excellent lead for further optimization and pre-clinical testing in the setting of CNS diseases.

Phosphodiesterases (PDEs) are a family of enzymes that catalyze the hydrolysis of the secondary signal messengers, cyclic adenosine monophosphate (cAMP) and cyclic guanosine monophosphate (cGMP). Both cAMP and cGMP are essential components for cell signaling and are known to regulate the function of airway smooth muscle, inflammatory cells, and immune cells.[1, 2] PDEs in mammals have been characterized into at least 11 different families of isozymes (PDE1-PDE11) that differ in their selectivity and specificity for the hydrolysis of cAMP and cGMP.[3] Among them PDE4, PDE7, and PDE8 are cAMP specific while PDE5, PDE6, and PDE9 are cGMP specific.[4] PDE4 is expressed predominantly in inflammatory and immune cells including lymphocytes, macrophages, eosinophils, and neutrophils where it tightly regulates the intracellular concentrations of cAMP.[2] The critical role cAMP in regulating inflammatory and autoimmune processes makes PDE4 an attractive target for treating inflammatory diseases such as chronic obstructive pulmonary disorder (COPD), asthma, rheumatoid arthritis, and psoriasis.[2]

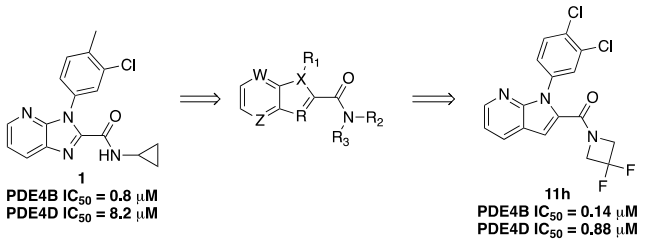

Figure 1. Modifications of known PDE4B inhibitor **1**, to new compound **11h**.

PDE4 exists in four known isoforms (PDE4A-D), among which PDE4A, B, and D are widely expressed in the brain.[5] Inhibition of PDE4 has been shown to have anti-inflammatory and anti-psychotic effects in various preclinical models.[2] In addition to inflammatory processes, PDE4B has been implicated in a number of other therapeutic roles, such as cancer[6], Alzheimer's disease[5], addiction[7-9], and Parkinson's disease.[10] The pan-PDE4 inhibitors such as roflumilast and apremilast have been approved for the treatment of COPD and psoriatic arthritis. Rolipram, another non-selective PDE4 inhibitor, was developed as a potential treatment for depression but its clinical use was abandoned due to a narrow therapeutic index.[11] However, these drugs have been hampered by dose limiting gastrointestinal side effects, such as nausea and emesis. These side effects are hypothesized to be partially associated with the inhibition of PDE4D isoform.[12] Hence there is an urgent need for developing novel chemical scaffolds that are brain penetrant and have preferential PDE4B binding. In this paper, we describe the synthesis, docking studies, and pharmacological and biological profile of a series of 1*H*-pyrrolo[2,3-*b*]pyridine-2-carboxamide derivatives as selective and potent PDE4B inhibitors.

We first wanted to evaluate the 5,6-core structure of the previously reported PDE4B inhibitor, **1** (PDE4B IC_{50} = 0.8 μM).[13] All of the synthesized compounds were initially evaluated for their *in vitro* inhibitory activity against PDE4B using rolipram as a positive control. Table 1 comprises the *in vitro* results of inhibitory activity against PDE4B for the title compounds under study, expressed as IC_{50} values and (%) inhibition in parenthesis. A number of variants were synthesized (see Experimental Section) and evaluated in an enzymatic PDE4B and PDE4D assay (BPS Biosciences, San Diego, CA) for activity. Our aim of this initial SAR evaluation was to systematically evaluate the nitrogen atom and their placement within the 5,6-framework in order to get a better understanding of the potency contributions of these atoms. The first compound, pyrazolo[1,5-*a*]pyridine **2**, showed some activity against PDE4B, however, there was an ~5-fold loss of

potency compared to **1** (**2**, IC_{50} = 4.2 μM). Replacing the imidazole moiety with a thiophene (**3**, thieno[2,3-*b*]pyrazine) led to an inactive compound. Removing the 6-membered ring nitrogen to afford the 1*H*-benzo[*d*]imdazole **4** led to an ~3-fold loss of activity (IC_{50} = ~2.4 μM), and further deletion of the imidazole nitrogen leaving the indole **5** led to an inactive compound. Interestingly, moving to the pyrrolo[2,3-*b*]pyridine, **7**, led to an increase in potency (PDE4B IC_{50} = 0.48 μM). Lastly, the *N*-methylated pyrrolo[3,2-*b*]pyridine, **6**, was not active. This is an interesting result as compounds such as this with a further cyclic ring between the pyrrole nitrogen and the amide have been reported as potent PDE4B inhibitors.

Table 1: Identification of the initial lead compound (1-7).

Cmpd	Structure	IC_{50}, nM; (% Inhibition @ 10 μM) PDE4B	PDE4D
1	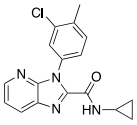	800	~8,200
2	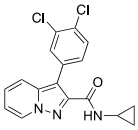	4,200	(21)
3	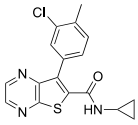	(46)	(21)
4	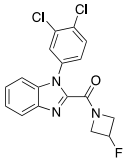	~2,400	~2,000
5	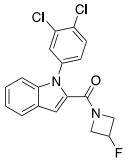	(58)	(31)
6	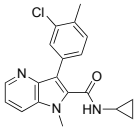	(56)	(27)
7	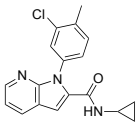	480	(41)
Rolipram		110	110

[a]PDE4 assays run at BPS Biosciences, San Diego, CA, n = 2.

Having identified the pyrrolo[2,3-*b*]pyridine, **7**, as a productive replacement, we further elaborated this ring system in order to fully vet this ring system. The analogs in Tables 2 and 3 were synthesized from common intermediates as shown in Scheme 1. The final compounds **11a-o** were synthesized starting from the common intermediate **8**, followed by Chan-Lam coupling to yield **9**.[14] Next, saponification of the ester led to the acid, **10**, which was then reacted with a variety of amines under standard coupling conditions (T3P, DIPEA) to yield the final compounds **11a-o**.[15] The second set of targets, **14a-w**, were synthesized in a similar fashion, but with a reversal of the steps. Initial saponification of the ester in **8**, followed by amide coupling (T3P, DIPEA) led to the penultimate compound **13**. Final targets, **14a-w**, were isolated after Chan-Lam coupling ($Cu(OAc)_2$, pyridine).[14]

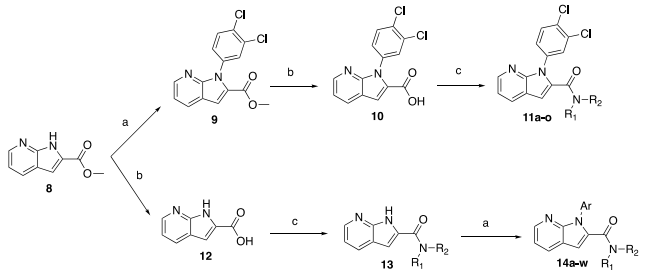

Reagents and conditions: a. $Cu(OAc)_2$, $ArB(OH)_2$ pyridine, CH_2Cl_2, rt, 12 h; b. NaOH, $MeOH \cdot H_2O$; c. T3P, NHR_1R_2, DIPEA, DMF, rt, 30 min to 4 h

Scheme 1. Synthesis of the final target compounds.

In Table 2, we explored the substitution effects of the amide portion of the 1*H*-pyrrolo[2,3-*b*]pyridine series of compounds by holding the 3,4-dichlorophenyl northern portion constant. It can be seen from the IC_{50} values that most of the 1*H*-pyrrolo[2,3-*b*]pyridine derivatives showed moderate to good inhibition against PDE4B (IC_{50} ranges from 0.11 – 1.1 μM, % inhibition of 99 – 20% at 10 μM). Careful analysis of the SAR (entries **11a-o**) reveals the importance of ring size and extent of hydrophobicity on the overall activity and selectivity against PDE4B over PDE4D. Our first analogs explored secondary amides with small aliphatic cyclic or methyl furan groups. The cyclopropyl, **11a**, and 3-fluorocyclobutane, **11c**, both retained activity against PDE4B (IC_{50} = 0.63 and 0.6 μM, respectively), and were selective for PDE4D (<50% inhibition at 10 μM, the term selective is applied to compound <50% inhibition). The cyclobutyl, **11b**, difluorocyclobutyl, **11d**, as well as the methylfuran, **11e**, were all much less active or inactive. Moving to a tertiary amide (cyclic amide) was a more productive substitution pattern. By replacing the NH-cyclobutyl in **11b** with the direct azetidine, **11f**, an ~10-fold increase in activity against PDE4B (IC_{50} = 0.11 μM) was observed. This increase in PDE4B activity was also accompanied by an increase in PDE4D activity (IC_{50} = 0.45 μM). Addition of a single fluorine (3-fluoroazetidine, **11g**) or a difluorine (3,3-difluoroazetidine, **11h**) also produced potent compounds with varying degrees of selectivity against PDE4D. The mono-fluoro, **11g**, showed some selectivity against PDE4D (PDE4B IC_{50} = 0.23 μM and 77% inhibition of PDE4D at 10 μM), whereas the difluoroazetidine was ~6-fold selective for PDE4B (PDE4B IC_{50} = 0.14 μM vs. PDE4D IC_{50} = 0.88 μM). Elongation of the tertiary amide by incorporation of a 3-trifluoromethyl group also produced an active compound (**11i**, PDE4B IC_{50} = 0.43 μM), but with only an ~2-fold selectivity versus PDE4D. Further elaboration of the amide space with a series of spirocyclic rings (entries **11j-m**) only exhibited moderate to weak inhibition against PDE4B. Introduction of a basic nitrogen in the spirocyclic ring (entries **11n-o**) lead to a significant loss of activity against PDE4B and PDE4D. This

may be due to lower lipophilic binding compared to **11j** and unfavorable interactions due to steric hindrance in the catalytic site of the enzyme. In this series, we were able to identify a novel scaffold **11h** bearing a 3,3-difluroazetidine ring, which exhibited higher inhibitory activity (0.14 μM) and 6-fold selectivity over PDE4D than its corresponding analogs. This compound was comparable in activity to the standard compound, rolipram, and was more selective versus PDE4D.

Table 2. SAR with variations at the R_1 group, 11a-o.

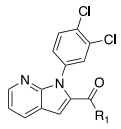

Cmpd	R_1	IC_{50}, nM; (% Inhibition @ 10 μM)[a]	
		PDE4B	PDE4D
11a		630	(59)
11b		1,100	(24)
11c		600	(36)
11d		(23)	(11.6)
11e		(70)	(52)
11f		110	450
11g		230	(77)
11h		140	880
11i		430	1,000
11j		(73)	(39)
11k		(39)	(17)
11l		(50)	(29)
11m		980	~2,300
11n	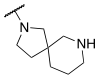	(20)	(6)
11o		(33)	(13)
Rolipram		110	110

[a]PDE4 assays run at BPS Biosciences, San Diego, CA, n = 2.

Based on the above results, we further evaluated a combination of aryl and amide substituents on the 1*H*-pyrrolo[2,3-*b*]pyridine ring system to develop more potent and selective PDE4B inhibitors. The aryl groups were chosen based on the activity in the originally reported series.[13] In entries **14a-c**, when R was 3-chloro-4-methylphenyl, increasing the size of the amide led to a decrease in activity by ~2-20 fold, similar to that seen previously. However, moving to the 3-fluoroazetidine, **14d**, did not produce the same improvement in potency as above, but this seemed to be an anomaly. When evaluating other R groups (4-chloro-3,5-difluorophenyl, **14f-i**, 4-cyano-3,5-difluorophenyl, **14j-o**, 4-chloro-3-fluorophenyl, **14s-v**), PDE4B activity was improved by using the 3-fluoroazetidine tertiary amide. In order to fully investigate the effect of R substitution on the core ring, we explored a series of heteroaryl groups while keeping R_1 (3-fluoroazetidine) constant as shown in entries **14w-z,bb**, Table 3. These heteroaryl substituents indicate that substituted pyridyl (entries **14x** and **14z**) retains activity against PDE4B (IC_{50} = 0.49 and 0.98 μM, respectively); although the activity is less than the **11h**. Interestingly, the 3-fluoro-4-methoxyphenyl group, **14y**, lost activity against PDE4B; however, the activity could be regained by the addition of an additional fluorine (3,5-difluoro-4-methoxyphenyl, **14bb**, IC_{50} = 0.41 μM). This compound also showed ~15-fold selectivity versus PDE4D. To our surprise, the 3,3-difluoroazetidine moiety (i.e., **11h**) that provided the best compound previously, was not a productive moiety in this new group of compounds (e.g., **14e** and others). Lastly, a methylene spacer was introduced between the phenyl group and the pyrrole (benzyl) and this change led to an inactive compound (**14w**).

Table 3: SAR with variations at both R and R_1 group (14a-w).

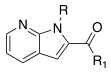

Cmpd	R	R_1	IC_{50}, nM; (% Inhibition @ 10 μM)	
			PDE4B	PDE4D
14a			480	(41)
14b		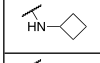	2,300	(43)
14c		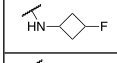	9,400	(25.6)
14d		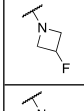	910	(60)
14e			(47)	(26)
14f			1,400	(53)

14g			1,300	(10.7)
14h			210	(62)
14i			(48)	(27)
14j			1,400	(18.5)
14k			1,800	(16.6)
14l		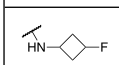	(58)	(12.1)
14m			(47)	(18)
14n			430	(66)
14o			(41)	(27)
14p	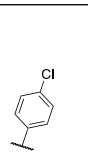		2,900	(10.1)
14q			5,000	(28.2)
14r			(47)	(25)
14s			970	(24)
14t			1,300	(39)
14u			610	(71)
14v			(48)	(25)
14w	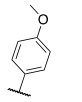		(67)	(37)
14x	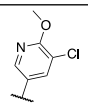		490	1,600
14y	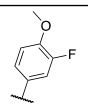		(77)	(52)
14z			980	~1,900

14aa			(37)	(20)
14bb	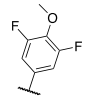		410	~6,300
14cc			(35)	(25)
14dd	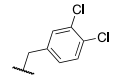		(72)	(58)
Rolipram			110	110
[a]PDE4 assays run at BPS Biosciences, San Diego, CA, n = 2.				

In order to gain an understanding of the structural basis for the SAR observed, we also studied the binding of the synthesized inhibitors through computational modeling. The 3D structure of the PDE4B was taken from a Protein Data Bank entry (PDB: 4X0F) having the ligand rolipram in place. Docking studies were performed using Maestro 11.0 (Schrödinger, Small-Molecule Drug Discovery Suite 2018-3) software using PDE4B in complex with (*R*)-(–)-rolipram as the starting point. The optimized ligands were docked using Glide software in Maestro 11.0. The resulting structures were then analyzed using pose viewer to identify specific contacts between ligand and receptors. As shown in Figure 2 (top), the primary SAR study and docking results suggested that entry **11h** core ring shows π-π stacking interactions with residues Phe618 and Tyr405. The azetidine ring extends into the catalytic domain to block the access of cAMP thereby laying the foundation for PDE4B inhibition. The docking results were also consistent with the observed SAR studies. Smaller groups like cyclopropyl/difluoroazetidine occupy the smaller pocket in the catalytic domain while larger spirocyclic groups at this position lead to steric hindrance and therefore unfavorable interactions leading to significant loss of PDE4B inhibitory activity.

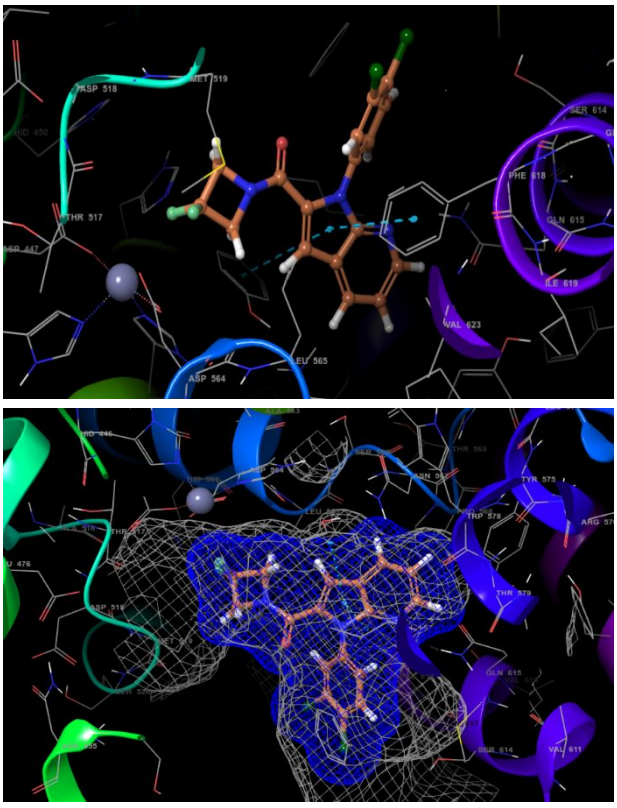

Figure 2. Predicted binding mode of pyrrolo[2,3-*b*]pyridine inhibitor 11h in the active site of PDE4B structure (PDB code 4X0F).

Since PDE4 inhibitors have well-documented anti-inflammatory properties[2], we evaluated the ability of these compounds to inhibit macrophage pro-inflammatory activity by measuring the production of the classical pro-inflammatory cytokine TNF-α (Figure 3). Two well-characterized pro-inflammatory stimuli were tested, namely lipopolysaccharide (LPS) and a synthetic lipopeptide (Pam3Cys) that represent prototypical bacterial ligands for Toll-like receptors 4 and 2, respectively (TLR4 and TLR2).[16] All of the test compounds inhibited TNF-α production by mouse bone marrow-derived macrophages to the same extent, or better than, the well-characterized PDE4 inhibitor, rolipram (Figure 3). A dose-dependent response was observed with regard to LPS-induced TNF-α release, where higher concentrations were less effective across the group of compounds (Figure 3A), a phenomenon which has been reported with other PDE4 inhibitors.[17] A similar dose-response was observed with some compounds when macrophages were stimulated with Pam3Cys (Figure 3B); nevertheless, cytokine production was significantly reduced across the compound class. None of the compounds elicited TNF-α production when tested alone (data not shown). It is noted that the compounds are all equally active in this assay, and this is an effect we are currently investigating. Collectively, these findings support the biological action of the target compounds, which model the anti-inflammatory actions of the well-characterized PDE4 inhibitor rolipram.[18]

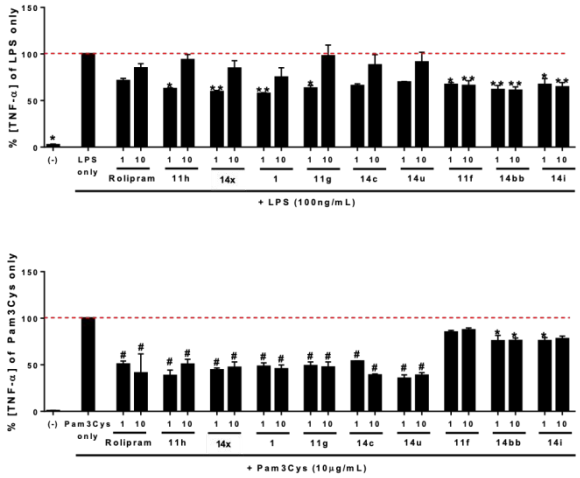

Figure 3. Target compounds inhibit macrophage pro-inflammatory activity. Bone marrow-derived macrophages were unstimulated (-) or pre-treated with the indicated concentrations of the well-characterized PDE4 inhibitor rolipram or target compounds (1 or 10 μM) for 30 min prior to LPS (100 ng/ml; A) or Pam3Cys (10 μg/ml; B) stimulation. After a 24 h treatment period, conditioned medium was collected to quantitate TNF-α expression by ELISA. Results are reported as the mean values (± SD) from 3 independent replicates for each treatment and were repeated in two separate experiments. *, $p < 0.05$; **, $p < 0.01$; #, $p < 0.0001$; One-way ANOVA with Dunnett's multiple comparisons post-hoc analysis.

Finally, having identified new PDE4 inhibitors, we next evaluated select compounds in a battery of Tier 1 *in vitro* DMPK assays (Table 4). A number of compounds evaluated displayed low (Q_H <25%) clearance in both human and mouse microsomes (**14x, 14z, 14bb**) and several other compounds displayed moderate clearance (**14i**, **14j**) in microsomes (Q_H <50%). In addition to showing low clearance, both pyridine containing compounds (**14x**, **14z**) displayed an excellent free fraction profile. In fact, most of the compounds evaluated had free fraction >3% in both species, with the exceptions of **11a** and **14a** in mice plasma (<1%).

Table 4. *In vitro* DMPK of selected compounds.

	Intrinsic Clearance (mL/min/kg)[a,b]				Plasma Protein Binding ($\%f_u$)[a,c]	
	Human		Mouse			
Cmpd	CL_{INT}	CL_{HEP}	CL_{INT}	CL_{HEP}	Human	Mouse
1	29.6	12.3	149.5	56.2	8.5	5.6
11a	178.6	18.8	157.4	57.3	2.6	0.6
11f	194.3	19.0	1213.7	83.8	3.9	3.0
11h	97.1	17.3	100.0	47.4	3.8	2.7

11i	295.6	19.6	1142.5	83.5	2.3	2.2
14a	172.5	18.7	551.4	77.4	1.1	0.6
14i	33.3	12.5	104	48.2	11.3	5.1
14j	31.5	12.6	<49.5	<31.9	23.5	9.6
14x	<23.1	<11	133.7	53.8	4.9	6.6
14z	<23.1	<11	<49.5	<31.9	47.4	39.3
14bb	<23.1	<11	<49.5	<31.9	30.2	13.3

Stability in Human Hepatocyte S9 Fractions

	$t_{1/2}$ (min)	CL_{HEP} (mL/min/kg)	ER
11h	49.4	12.6	0.63

[a]*In vitro* DMPK studies performed at Q2 Solutions, Indianapolis, IN [b]Intrinsic and predicted hepatic clearance based on experiments in liver microsomes. [c]%f_u = % fraction unbound

Lastly, we profiled **11h** against a wider panel of PDE isoforms (see Supplemental Tables 1) in a radioligand binding assay for % inhibition at 10 μM. **11h** was selective against all of the isoforms tested (<50% inhibition), except PDE3B (87% inhibiton. In addition, **11h** was also tested in the NIMH Psychoactive Drug Screening Program (PDSP), which tests compounds against a wide panel of targets (see Suppl. Table 2).[19] In this panel, **11h** was not active (<50% inhibition) against all receptors except 5-HT_{2C} (59% inhibition) and σ2 (70% inhibition). However, follow-up IC_{50} determinations showed **11h** was only weakly active (5-HT_{2c}, IC_{50} >10 μM and σ2, IC_{50} = 7.8 μM)

In summary, a scaffold-hopping experiment identified a novel 1*H*-pyrrolo[2,3-*b*]pyridine-2-carboxamide series of PDE4B inhibitors. The compounds display a range of PDE4B inhibition and selectivity versus PDE4D. In addition, we have shown using molecular modeling how these compounds interact with the enzyme. We have also shown that our compounds are equipotent with rolipram in cellular assays inhibiting macrophage pro-inflammatory cytokine activity. Finally, compounds also show good *in vitro* PK profiles. Further optimization and *in vivo* activity are on-going and will be reported in due course.

ASSOCIATED CONTENT

Supporting Information

The Supporting Information is available free of charge on the ACS Publications website.

General methods for the synthesis and characterization of all compounds, methods for the cellular assay and selectivity data (PDF)

AUTHOR INFORMATION

Corresponding Author

*Phone: 1 402-559-9729. Fax: 1 402-559-5643. E-mail: corey.hopkins@unmc.edu

Author Contributions

C.R.H., T.K. drafted and corrected manuscript with input from all authors. A.K.V., C.D.A. and S.S. performed the chemical synthesis and C.R.H. oversaw the medicinal chemistry, target selection and interpreted the biological data. A.K.V. performed the molecular modeling. A.L.A. and C.E.H. performed the macrophage cellular assays and T.K. oversaw the experiments. S.K. and N.G. performed the PK studies. Y.A. oversaw all of the PK experiments.

Funding Sources

C.R.H. thanks the UNMC College of Pharmacy for start-up funds.

ACKNOWLEDGMENT

The authors would like to thank Q2 solutions for the *in vitro* DMPK experiments, BPS Biosciences for the PDE4 *in vitro* experiments, and Frontage Laboratories for the *in vivo* PK experiments. The authors would also like to thank Prof. Daryl J. Murry for the high-resolution mass spectrometry data.

ABBREVIATIONS

PDE4, phosphodiesterase 4; K_p, total brain:plasma ratio, T3P, propylphosphonic anhydride; DIPEA, diisopropylethyl amine, DMF, dimethylformamide; AUC, area under the curve; TNF, tumor necrosis factor; ELISA, enzyme-linked immunosorbent assay; PK, pharmacokinetics; DMPK, drug metabolism and pharmacokinetics.

REFERENCES

(1) Houslay, M. D., Schafer, P., Zhang, K. Y. J. Keynote review: Phosphodiesterase-4 as a therapeutic target. *Drug Disc. Today* **2005**, *10*, 1503-1519.

(2) Sakkas, L. I., Mavropoulos, A., Bogdanos, D. P. Phosphodiesterase 4 inhibitors in immune-mediated diseases: mode of action, clinical applications, current and future perspectives. *Curr. Med. Chem.* **2017**, *24*, 3054-3067.

(3) Fertig, B. A., Baillie, G. S. PDE4-mediated cAMP signalling. *J. Cardiovasc. Dev. Dis.* **2018**, *5*, 8.

(4) Ahmad, F., Murata, T., Simizu, K., Degerman, E., Maurice, D., Manganiello, V. Cyclic nucleotide phosphodiesterases: important signaling modulators and therapeutic targets. *Oral Dis.* **2015**, *21*, e25-e50.

(5) Wu, Y., Li, Z., Huang, Y.-Y., Wu, D., Luo, H.-B. Novel phosphodiesterase inhibitors for cognitive improvement in Alzheimer's disease. *J. Med. Chem.* **2018**, *61*, 5467-5483.

(6) Savai, R., Pullamsetti, S. S., Banat, G.-A., Weissmann, N., Ghofrani, A., Grimminger, F., Schermuly, R. T. Targeting cancer with phosphodiesterase inhibitors. *Expert Opin. Investig. Drugs* **2010**, *19*, 117-131.

(7) Heckman, P. R. A., Blokland, A., Bollen, E. P. P., Prickaerts, J. Phosphodiesterase inhibition and modulation of corticostriatal and hippocampal circuits: clinical overview and translational considerations. *Neurosci. Biobehav. Rev.* **2018**, *87*, 233-254.

(8) Wen, R.-T., Feng, W.-Y., Liang, J.-H., Zhang, H.-T. Role of phosphodiesterase 4-mediated cyclic AMP signaling in pharmacotherapy for substance dependence. *Curr. Pharm. Des.* **2015**, *21*, 355-364.

(9) Olsen, C. M., Liu, Q.-S. Phosphodiesterase 4 inhibitors and drugs of abuse: current knowledge and therapeutic opportunities. *Front. Biol.* **2016**, *11*, 376-386.

(10) Knott, E. P., Assi, M., Rao, S. N. R., Ghosh, M., Pearse, D. D. Phosphodiesterase inhibiors as a therapeutic approach to neuroprotection and repair. *In. J. Mol. Sci.* **2017**, *18*, 696.

(11) Prickaerts, J., Heckman, P. R. A., Blokland, A. Investigational phosphodiesterase inhibitors in phase I and phase II clinical trials for Alzheimer's disease. *Expert Opin. Investig. Drugs* **2017**, *26*, 1033-1048.

(12) Zhang, C., Xu, Y., Zhang, H.-T., Gurney, M. E., O'Donnell, J. M. Comparison of the pharmacological profiles of selective PDE4B and PDE4D inhibitors in the central nervous system. *Sci. Rep.* **2017**, *7*, 40115.

(13) Chappie, T. A., Verhoest, P. R., Patel, N. C., Hayward, M. M., Azabenzimidazole compounds, **2014**, US2014/0235612 A1, 54.

(14) Lam, P., Clark, C., Saubern, S., Adams, J., Wingers, M., Chan, D., Combs, A. New aryl/heteroaryl C-N bond cross-coupling reactions via arylboronic acid/cupric acetate arylation. *Tetrahedron Lett.* **1998**, *39*, 2941-2944.

(15) Dunetz, J. R., Xiang, Y., Baldwin, A., Ringling, J. General and scalable amide bond formation with epimerization-prone substrates using T3P and pyridine. *Org. Lett.* **2011**, *13*, 5048-5051.

(16) Kawasaki, T., Kawai, T. Toll-like receptor signaling pathways. *Front. Immunol.* **2014**, *5*, 461.

(17) Aldrich, A., Bosch, M. E., Fallet, R., Odvody, J., Burkovetskaya, M., Rama Rao, K. V., Cooper, J. D., Drack, A. V., Kielian, T. Efficacy of phosphodiesterase-4 inhibitors in Juvenile Batten Disease (CLN3). *Ann. Neurol.* **2016**, *80*, 909-923.

(18) Jin, S. L., Lan, L., Zoudilova, M., Conti, M. Specific role of phosphodiesterase 4B in lipopolysaccharide-induced signaling in mouse macrophages. *J. Immunol.* **2005**, *175*, 1523-1531.

(19) Besnard, J., Ruda, G. F., Setola, V., Abecassis, K., Rodriquiz, R. M., Huang, X.-P., Norval, S., Sassano, M. F., Shin, A. I., Webster, L. A., Simeons, F. R. C., Stojanovski, L., Prat, A., Seidah, N. G., Constam, D. B., Bickerton, G. R., Read, K. D., Wetsel, W. C., Gilbert, I. H., Roth, B. L., Hopkins, A. L. Automated design of ligands to polypharmacological profiles. *Nature* **2012**, *495*, 215-220.

Authors are required to submit a graphic entry for the Table of Contents (TOC) that, in conjunction with the manuscript title, should give the reader a representative idea of one of the following: A key structure, reaction, equation, concept, or theorem, etc., that is discussed in the manuscript. Consult the journal's Instructions for Authors for TOC graphic specifications.

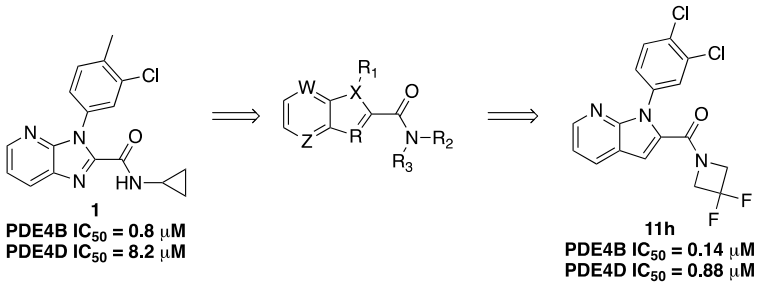

Keywords: PDE4, phosphodiesterase, CNS diseases, pyrrolo[2,3-*b*]pyridine